



ELSEVIER

Journal of Chromatography A, 832 (1999) 149–163

JOURNAL OF  
CHROMATOGRAPHY A

# Effect of electric field on liquid chromatographic separation of peptide digests

## Combining capillary separation techniques

Alex Apffel<sup>a,\*</sup>, Hongfeng Yin<sup>a</sup>, William S. Hancock<sup>a</sup>, Douglass McManigill<sup>a</sup>,  
John Frenz<sup>b</sup>, Shiao-Lin Wu<sup>c</sup>

<sup>a</sup>Hewlett-Packard Laboratories, 3500 Deer Creek Road, Palo Alto, CA 94304, USA

<sup>b</sup>Genentech Inc., 460 Point San Bruno Boulevard, South San Francisco, CA 94080, USA

<sup>c</sup>Scios Nova Inc., 2450 Bayshore Parkway, Mountain View, CA 94043, USA

Received 20 July 1998; received in revised form 11 November 1998; accepted 13 November 1998

### Abstract

A system is described which allows operation of a range of capillary based liquid phase separations including capillary electrophoresis, isocratic and gradient capillary electrochromatography, isocratic and gradient capillary liquid chromatography and electrically assisted gradient capillary liquid chromatography. The system was coupled to electrospray ionization mass spectrometry in the electrically assisted capillary liquid chromatography mode to investigate the effect of applied voltage on the selectivity in peptide mapping separations. Analyses were performed on tryptic digests of recombinant human growth hormone and tissue plasminogen activator. The results show a small but useful effect on selectivity that can be used to fine tune specific separations. © 1999 Elsevier Science B.V. All rights reserved.

**Keywords:** Electric field; Capillary electrochromatography; Peptides

### 1. Introduction

Considerable interest has been shown in the last several years in the development of capillary electrochromatography (CEC) [1,2], a separation technique carried out in packed capillaries in which the mobile phase liquid flow-rate is generated by electroosmotic flow processes rather than pressure driven pumping. Originally, CEC was considered to have a potentially major efficiency advantage over conventional HPLC by producing a plug-like flow profile as opposed to the conventional parabolic flow profile. Although the

actual flow dynamics have proved to be more complex than this simple model, a similar phenomenon has been found to occur on the micro-scale in inter-particle channels. For uncharged analytes, this has been shown to result in relatively high separation efficiency in short analysis times, using either isocratic or gradient elution techniques due to use of small diameter particles and improved dispersion properties. For charged species, the application of an electrical potential introduces an additional selectivity mechanism due to electrophoretic migration of the analytes.

Most recent work has focused on instrumental development, exploitation of the high efficiency of

\*Corresponding author.

the separations, or selectivity effects due to combined reversed-phase and electrophoretic mechanisms. In the current work, however, we focus exclusively on the use of axial electrical fields superimposed on pressure driven reversed-phase HPLC separations as a selectivity mechanism, a technique which has been termed electrically assisted capillary HPLC (electrically assisted cLC) or pseudo-electrochromatography (pEC). Specifically, we have focused on the application of pEC to the separation of proteolytic digests of proteins and glycoproteins. As a tool to identify selectivity effects on peptide mapping, an electrospray ionization interface has been developed for combination with electrically assisted cLC. In combination with reversed-phase gradient HPLC, it was found that the use of electrical fields can be continuously or selectively applied to fine tune separation selectivity.

## 2. Experimental

### 2.1. Apparatus

Separations were controlled and evaluated using

the apparatus shown schematically in Fig. 1. A HP 1600A HP<sup>3D</sup>CE (Hewlett–Packard, Palo Alto, CA, USA) was modified to enable a single platform approach to capillary electrochromatography, capillary HPLC or a combination of the two techniques, electrically assisted cLC without changing either sample introduction or detection processes. An HP1100 binary HPLC solvent delivery system was used to deliver pressure driven flow to the system. The HP<sup>3D</sup>CE MS interface cassette was modified to provide a flow splitter at the head of the packed capillary column, while two independently activated Rheodyne TPMV 6 port two position valves enabled either a split or splitless injection. Fused-silica capillaries, 100  $\mu\text{m}$  I.D.  $\times$  375  $\mu\text{m}$  O.D.  $\times$  various lengths (Polymicro Technologies, Phoenix, AZ, USA) were packed with Vydac 218TPB5 ( $C_{18}$ ) 5  $\mu\text{m}$ , 300  $\text{\AA}$  packing material (Phase Separations, Hesperia, CA, USA) using a modified version of the method described by Smith and Evans [3].

For electrically assisted cLC–MS, a similar system was used as shown in Fig. 2. In this configuration, the modified capillary cassette was not used and the separation capillary was not thermostated. A HP 5989B quadrupole mass spectrometer with and modi-

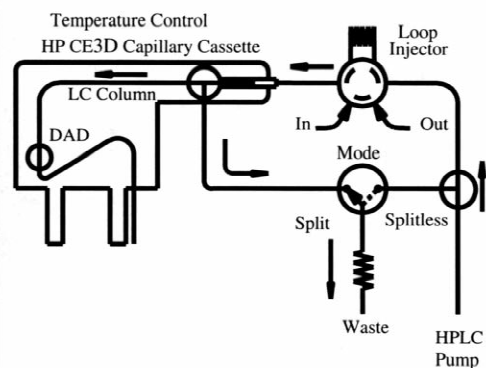
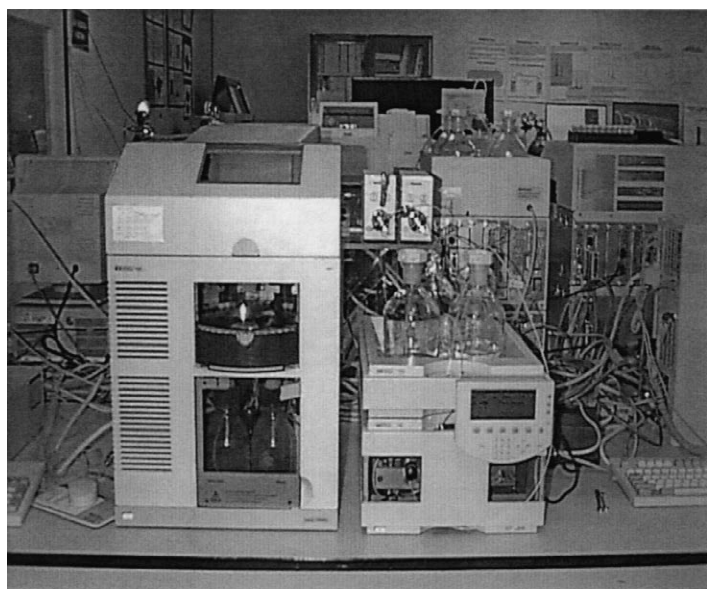


Fig. 1. Photograph and schematic of CEC apparatus.

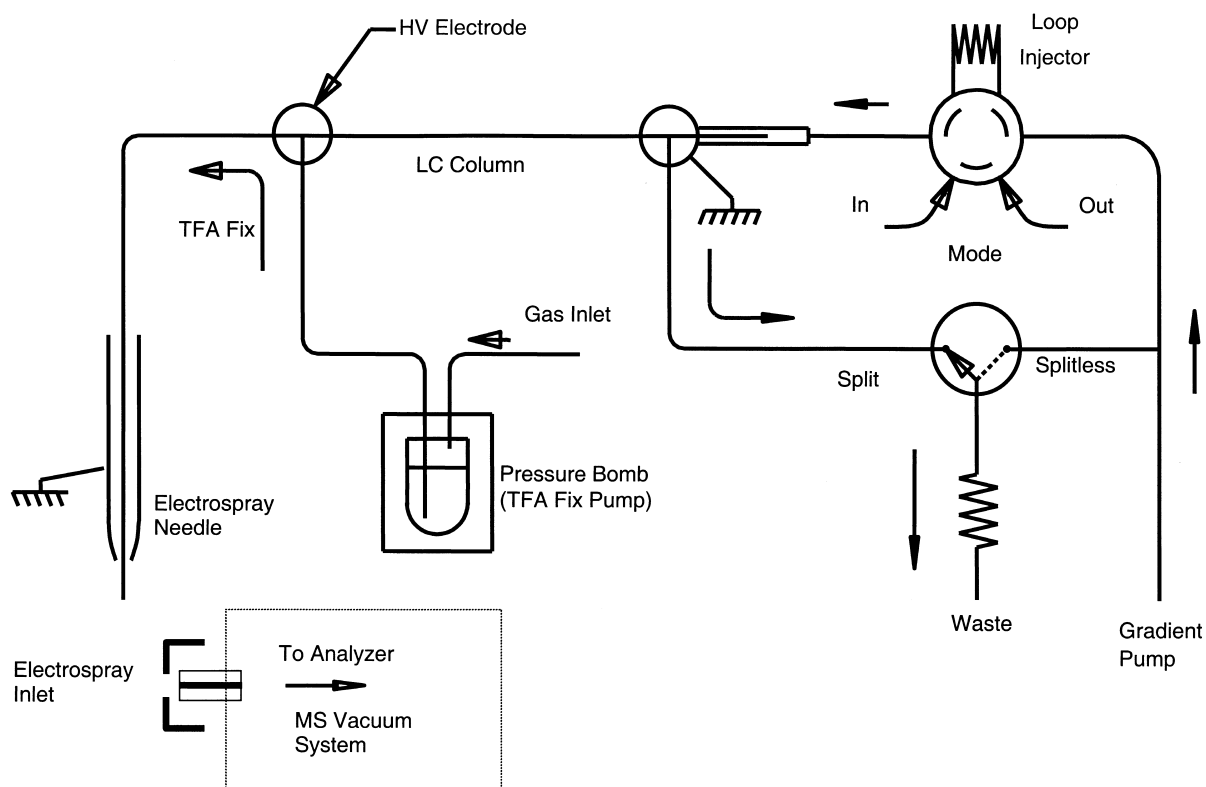


Fig. 2. Schematic of electrically assisted cLC-MS system.

fied HP 59987 electro spray source was used for mass spectral detection. The mass spectrometer was equipped with extended mass (2000 amu), high energy dynode detector (HED) and IRIS octapole ion guide (Analytica of Branford, Branford, CT, USA). A pressure reservoir providing both HV electrical connection to the column exit as well as post-column addition of a make-up flow of 50% acetic acid at 3–5  $\mu\text{l}/\text{min}$ . The post column addition [4] was used to counteract the signal suppression effects due to the trifluoroacetic acid containing mobile phase. The end of the separation column and the electro spray needle were connected via 50 cm  $\times$  20  $\mu\text{m}$  fused-silica capillary. The end of this capillary was carefully bevelled and painted with gold paint. The electro spray needle was operated in an orthogonal arrangement [5] with the tip of the 20  $\mu\text{m}$  capillary acting as the electro spray needle. Approximately 0.1 l/min nebulizing gas was introduced

coaxially. Under these conditions, the column inlet and electro spray needle were operated at ground potential while the pressure reservoir was operated at elevated voltage.

Instrument Control was accomplished using an HP Chemstation data system.

## 2.2. Chemicals and methods

HPLC Grade acetonitrile and 2-propanol, acetic acid, analyte and peptide standards were obtained from Sigma (St. Louis, MO, USA). Protein and Protein Digest samples were obtained courtesy of Genentech (South San Francisco, CA).

Column flow-rates were set using a fixed restrictor as shown in Fig. 1. Typical inlet flow-rates of 0.35 ml/min resulted in 1  $\mu\text{l}/\text{min}$  column flow. For model studies, isocratic separations were carried out using 90% 25 mM phosphate buffer at pH 2.5, 10%

acetonitrile pumped at approximately 1  $\mu$ l/min. For peptide mapping, typical conditions were 0–60% acetonitrile/60 min with a constant 0.1% TFA. At these low pH values, no appreciable electroosmotic flow resulted from applied voltage.

### 3. Results and discussion

#### 3.1. General operational characteristics

Using the instrument shown in Fig. 1, it was possible to perform separations in a number of operation modes, including split or splitless injection, isocratic or gradient elution and capillary HPLC, capillary electrochromatography or electrically assisted capillary HPLC. Examples of these different operating modes are shown in Fig. 3 for the separation of pthalates.

In terms of injection capabilities, a split injection is made by injecting a fixed volume at 0.2–0.4 ml/min and splitting the inlet flow at the column head (typically 100:1) by introducing a fixed restric-

tion down stream of the column head. Splitless injection could be accomplished by introducing the restriction and flow splitting prior to the injection loop. In this mode, the injection volume was determined by the time the injection valve was actuated and the injection loop was in the flow path. For either injection mode, following the transfer of sample to the column, the valving was changed to the “splitless” mode to reduce gradient delay volume. Splitless injection, in combination with gradient elution allows the injection of relatively large volumes of dilute samples in non-elutotropic solvents without a significant contribution to chromatographic dispersion.

In terms of separation modes, capillary HPLC was performed by splitting the flow from a gradient HPLC pump (operating in either gradient or isocratic conditions) and delivering the split flow to the capillary column in the absence of any applied potential. For capillary electrochromatography, the restriction after the column split was reduced such that the split ratio was essentially 1:0 and a voltage was applied across the column. Under these con-

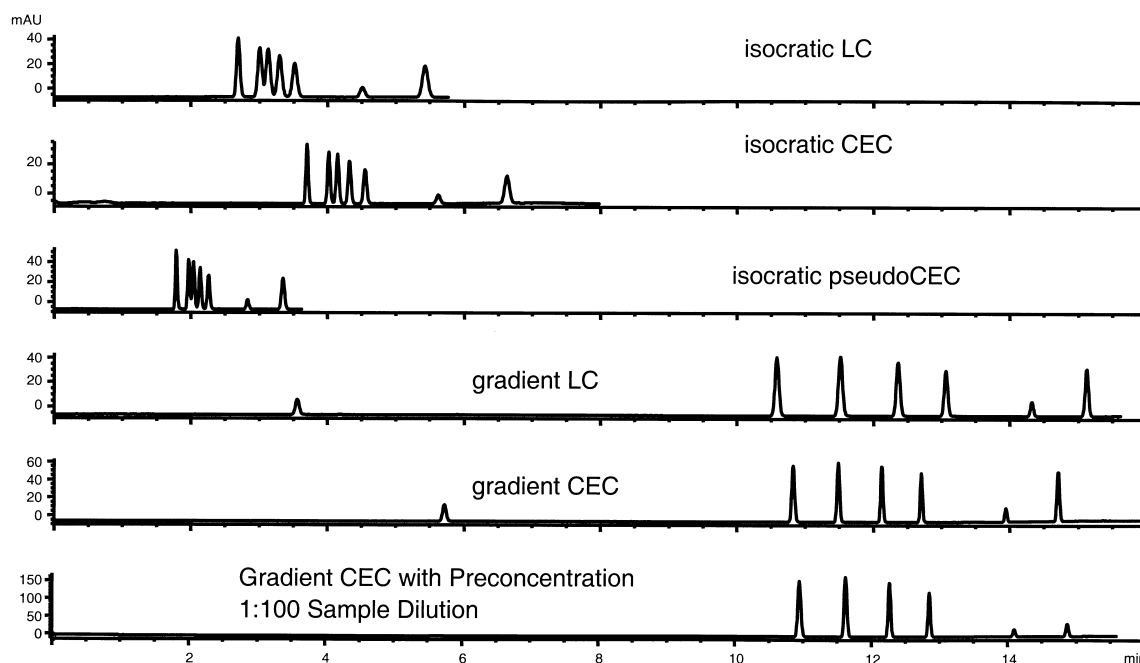


Fig. 3. Operation modes: Separation of parabens using various capillary separation modes. Column: 25 cm  $\times$  100  $\mu$ m I.D. 3  $\mu$ m CEC Hypersil C18. Mobile phase: isocratic: 10 mM MES pH 6.05 in 90% acetonitrile. Gradient 10 mM MES pH 6.05 40–90% acetonitrile/15 min.

ditions, the mobile phase was constantly refreshed at the head of the column, but there was no net pressure drop across the column and consequently, any flow through the column was due to electroosmotic flow. Electrically assisted capillary HPLC was accomplished by combining these two approaches. The column flow in this mode is the sum of pressure driven and electroosmotic flow.

### 3.2. Electrically assisted capillary HPLC of charged molecules

While a good deal of work has been done describing the behaviour of uncharged analytes in CEC, we wished to evaluate the effect of an electric field on

chromatographic selectivity of charged molecules. In order to isolate this effect the system was operated in a electrically assisted capillary HPLC mode at low pH under which conditions the electroosmotic flow could be essentially negated. Fig. 4 shows the separation of thiourea (uncharged) and phenylalanine (positively charged) under isocratic conditions with  $-20$ ,  $0$  and  $+20$  kV potential applied to the exit of the capillary. As one might expect, the retention of thiourea is unaffected, while the phenylalanine is accelerated by the negative potential (top frame) and retarded by positive potential (bottom frame) relative to the retention behavior at  $0$  potential (middle frame). When a similar experiment is performed under gradient conditions (Fig. 5), the results were considerably different. In this case, the samples was

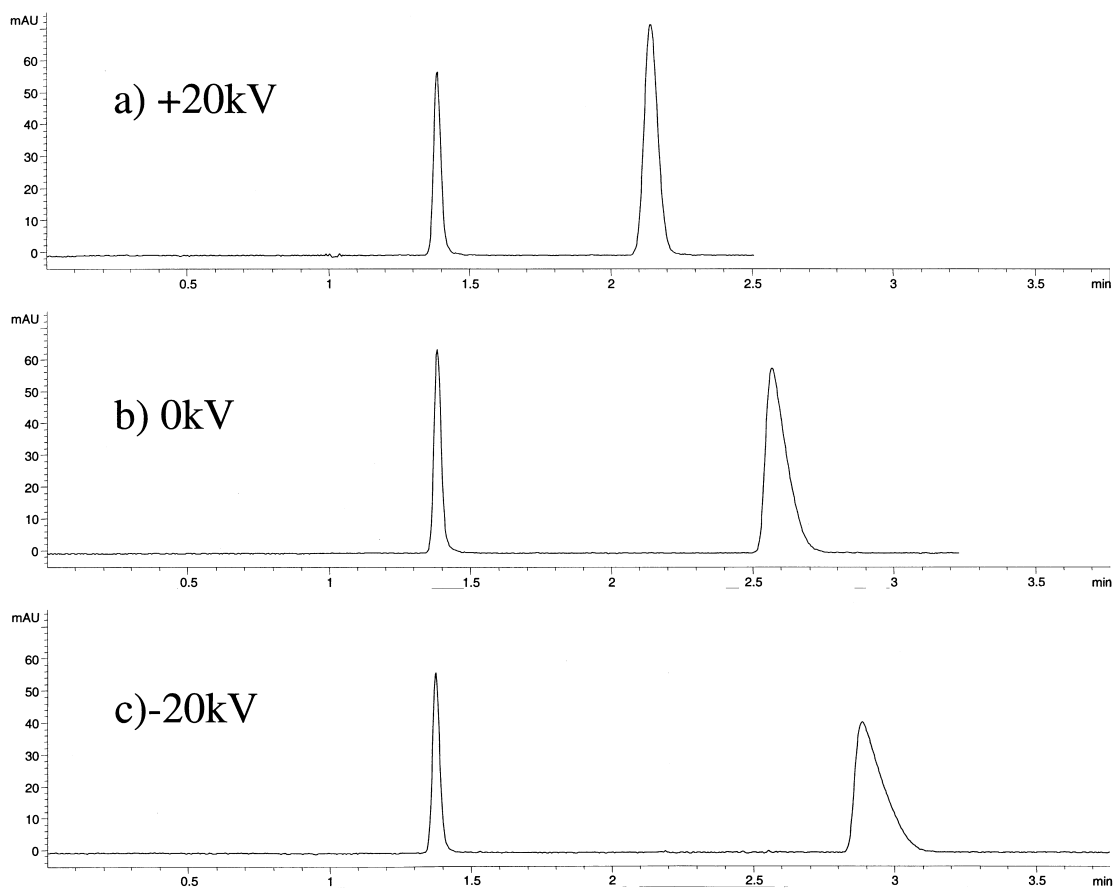


Fig. 4. Isocratic electrically assisted cLC. Separation of thiourea and phenylalanine. Column: 25 cm  $\times$  150  $\mu$ m I.D. 5  $\mu$ m Vydac C18. Mobile phase: 90% 25 mM phosphate buffer, pH 2.5; 10% acetonitrile.

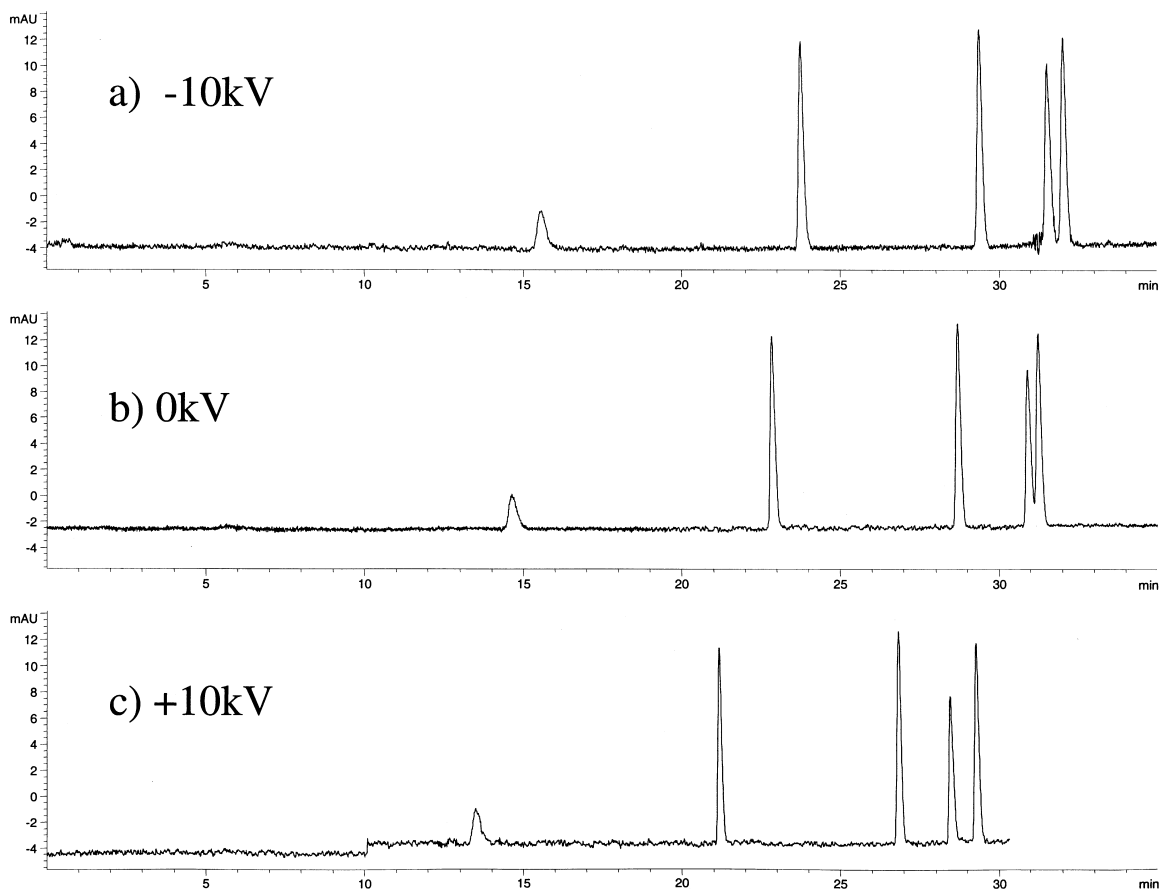


Fig. 5. Gradient electrically assisted cLC.. Separation of peptide mixture. (a)  $-10$  kV, (b)  $0$  kV, (c)  $10$  kV. Column:  $25$  cm  $\times$   $100$   $\mu$ m I.D.  $5$   $\mu$ m Vydac C18. Mobile phase A:  $0.05\%$  TFA/water. B:  $0.045\%$  TFA/acetonitrile. Gradient: initial  $0\%$  for  $5$  min;  $0$ – $35\%$  B/ $30$  min.

changed to a peptide standard, and it was found that although some change in selectivity did occur, the applied potential had far less impact on the separation than in the case of the isocratic separation.

To further investigate this difference, a step gradient experiment was performed using phenylalanine as a sample. Initial isocratic conditions were chosen such that the sample was fully retained on the column, and after  $7$  min, a step gradient was applied such that the analyte was rapidly eluted. This experiment was performed with  $0$  kV and  $-10$  kV applied voltage (Fig. 6). Noting an identical elution time for the sample under these two voltage conditions, it was postulated that the electric field had little effect on a

sample that was adsorbed to the stationary phase. A model was generated to describe this behavior.

$$V_{\text{avg}} = \frac{1}{1 + k'} (v_{\text{linear}} + \mu E) \quad (1)$$

As in chromatography, transport of an analyte can occur only when that analyte resides in the mobile phase. Although the average velocity may be low, the analyte is either adsorbed on the surface of the packing (zero velocity) or it is travelling with the velocity of the mobile phase ( $v_{\text{linear}}$ ). Since the applied field only effects the solute while it is in the mobile phase, then the mobile phase and electrophoretic velocity, to the first order, are additive.

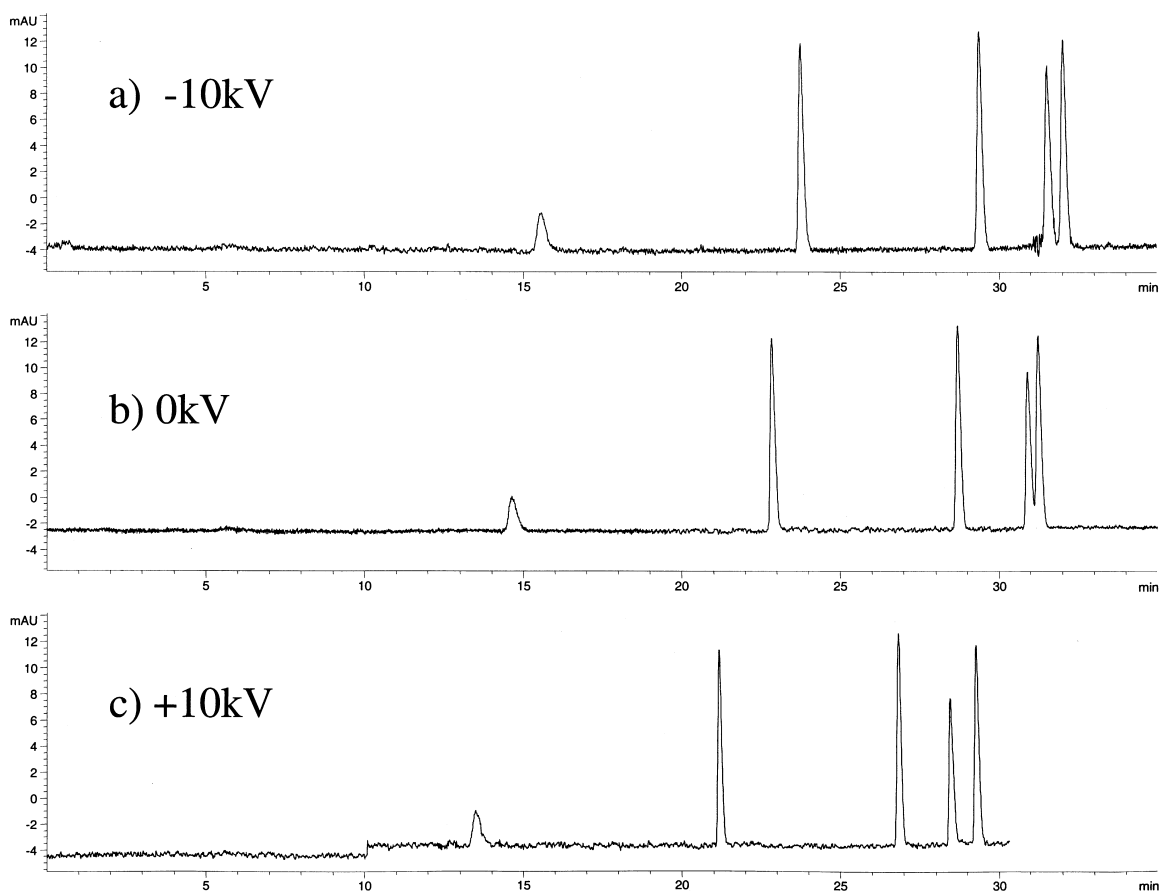


Fig. 6. Step gradient LC phenylalanine. Column: 25 cm×150  $\mu$ m I.D. 5  $\mu$ m Vydac C18. Mobile phase A: 0.05% TFA/water. B: 0.045%TFA/acetonitrile. Gradient as shown.

Thus, in so far as the analyte is either adsorbed, or travelling at the mobile phase velocity, the actual time spent in the mobile phase is  $t_0$  independent of the retention time.

$$\int_0^{t_r} \frac{1}{1+k(t)} dt = t_0 \quad (2)$$

Thus, depending on the gradient utilized, the residence time in the mobile phase ( $t_0$ ) can be very small relative to the total retention time. While this explains the relatively minor selectivity effects seen in gradient elution electrically assisted cLC, it also

suggests an approach to separation optimization as shown in Fig. 7 [6]. For two components, A and B, with differing retention times in a given gradient separation, Fig. 7 shows the amount of time the analyte spends in the mobile phase as a function of the total analysis time. If a potential were applied between times  $t_1$  and  $t_2$ , it would effect component A, with almost no effect on component B. This is particularly pronounced in separations involving peptides and proteins in which the retention mechanism is closer to a programmed desorption process than a continuous differential elution process [7]. Fig. 8 shows application of this approach to the separation of a tryptic digest of recombinant DNA

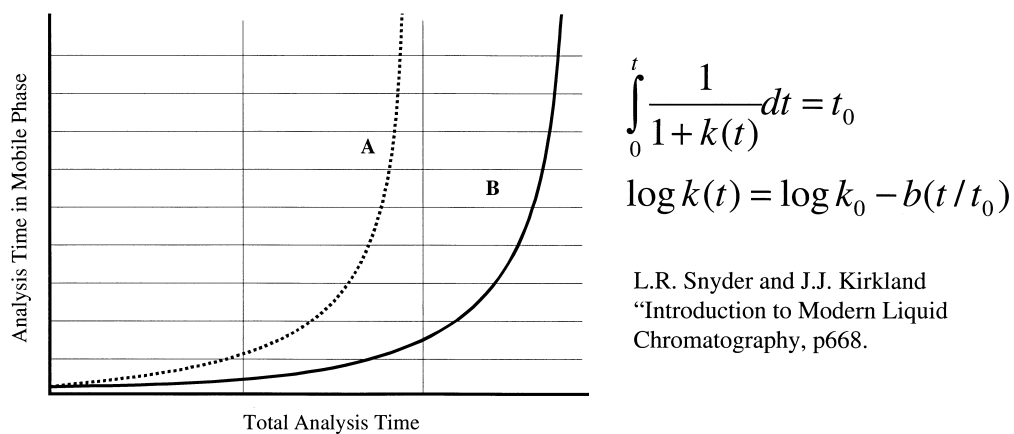


Fig. 7. Residence time in mobile phase versus total retention time. Adapted from Ref. [6].

derived human growth hormone (rhGH). The top panel shows no applied voltage while the bottom panel shows  $-15$  kV applied between 20 and 35 min. The retention and resolution during this period closely resembles the continuous voltage case, while the ranges before and after appear very similar to the 0 voltage case.

### 3.3. Electrically assisted cLC-MS

In order to investigate the correlation in complex peptide maps between peptide structure and selectivity effects of applied voltages in gradient electrically assisted cLC, it was necessary to utilize electrospray ionization mass spectrometry as a detection system.

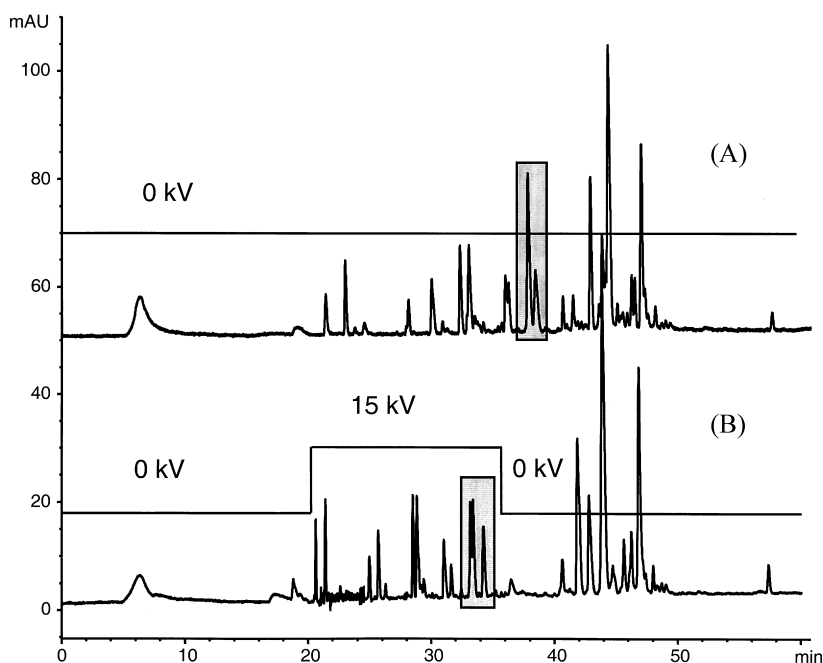


Fig. 8. Optimized electrically assisted cLC separation of rhGH tryptic; (A) no applied voltage; (B) optimized voltage program as shown. Digest column: 25 cm  $\times$  100  $\mu$ m I.D. 5  $\mu$ m Vydac C18. Mobile phase A: 0.05% TFA/water. B: 0.045% TFA/acetonitrile. Gradient: initial 0% for 5 min; 0–60%B/60 min.



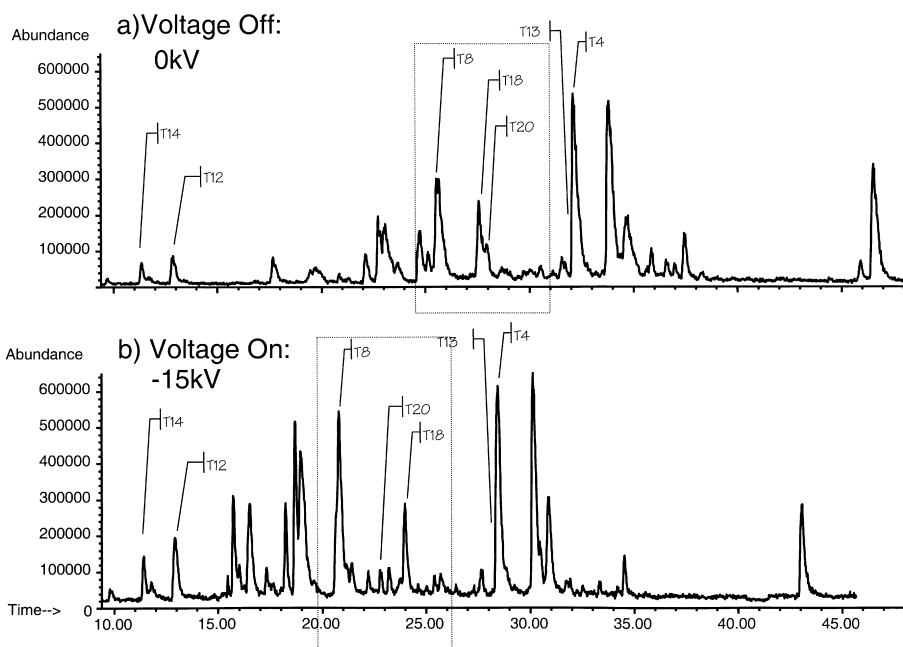


Fig. 9. Tryptic digest of rhGH by electrically assisted cLC-MS. Column: 25 cm $\times$ 100  $\mu$ m I.D. 5  $\mu$ m Vydac C18. Mobile phase A: 0.1% TFA/water. B: 0.09%TFA/acetonitrile. Gradient: initial 0% for 5 min; 0–60%B/60 min.

A modified configuration of the instrument was required for these experiments as shown in Fig. 2. Several features of this modification are worth noting. As the goal for this instrument was to investigate specific selectivity effects, it was not optimized with respect to extra column band

broadening and sensitivity. Firstly, in order to allow the HPLC gradient pump and the electrospray needle to operate at ground potential, the column exit was operated at elevated potential and connected via a zero dead volume Tee to a 50 cm $\times$ 20  $\mu$ m capillary to the electrospray inlet. The other arm of the tee

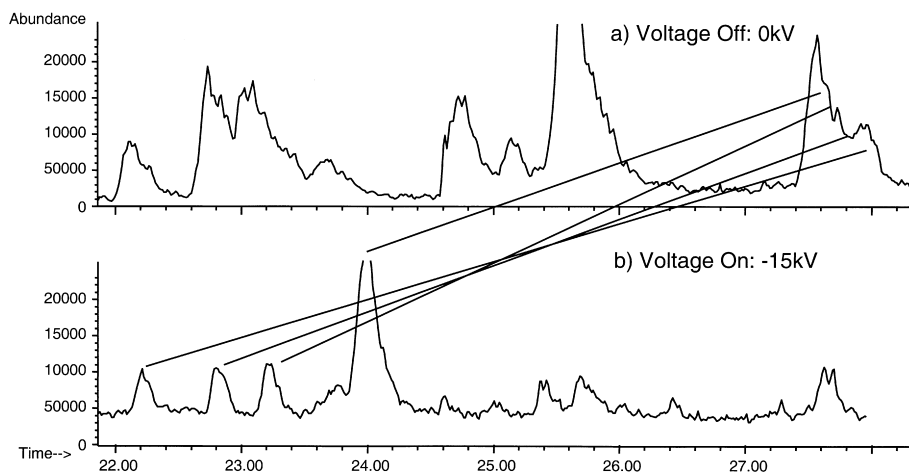


Fig. 10. Detail of Fig. 9.

was connected to a pressure reservoir bloop which supplied a post-column addition of 50% acetic acid/ acetonitrile to counter-act the signal suppressing effects of TFA containing mobile phases. Secondly, the separation column was not thermostated, which resulted in a mixture of joule heating and electrophoretic effects when voltage was applied. Finally, in order to minimize the distance (and consequently volume) between the column and the mass spectrometer, the UV–Vis detector was bypassed.

For the analysis of tryptic digests of recombinant DNA derived proteins, the known peptide sequence and the known proteolytic specificity of the digestion enzyme allow the prediction of expected peptide

fragments in the digest. The use of ESI-MS as a detector for the separation of the digest mixtures allows unequivocal correlation between peak retention and peptide sequence based on the detected mass of each component. The electrically assisted cLC–MS system was used to analyze a tryptic digest of recombinant DNA derived human growth hormone (rhGH) with and without applied voltage (Fig. 9). The application of voltage to the electrically assisted cLC–MS analysis results in a marked decrease in retention. A number of subtle selectivity effects were also observed, as shown in Fig. 10. In these data, the identity of specific peaks has been determined and tracked with the MS data. From

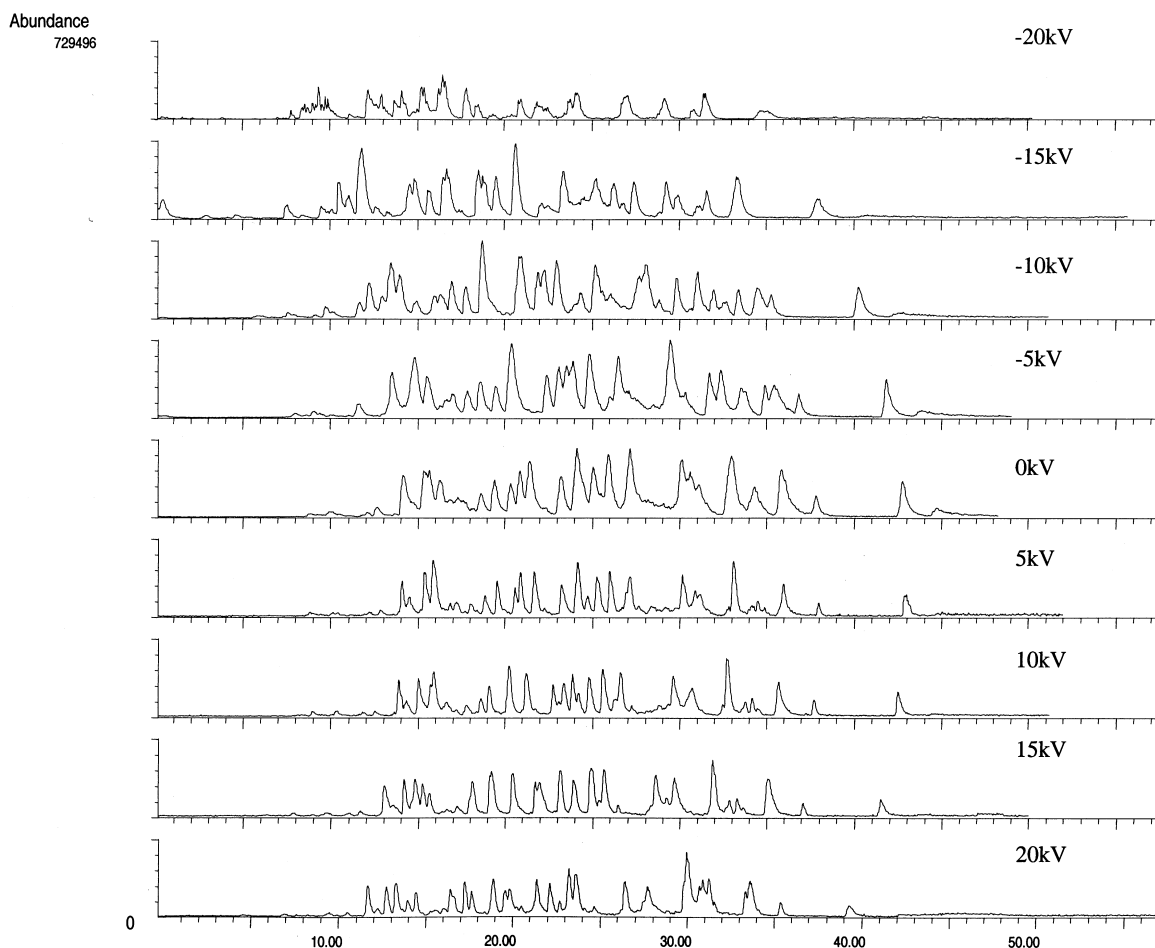


Fig. 11. Tryptic digest of rTPA by electrically assisted cLC–MS at various applied voltages. (a) –20 kV; (b) –15 kV; (c) –10 kV; (d) –5 kV; (e) 0 kV; (f) 5 kV; (g) 10 kV; (h) 15 kV; (i) 20 kV. Column: 25 cm  $\times$  100  $\mu$ m I.D. 5  $\mu$ m Vydac C18. Mobile phase A: 0.1% TFA/water. B: 0.09% TFA/acetonitrile. Gradient: initial 0% for 5 min; 0–60%B/60 min.

these results, although the use of superimposed voltage can be exploited for fine tuning of resolution, the effect is subtle and not yet simple to predict in the context of the entire map.

### 3.4. Selectivity effects in a complex glycoprotein map (rTPA)

Hancock et al. [8,9] have noted that changes in temperature can also result in changes in selectivity. The wide ranging selectivity effects are best illustrated with a very complex map and thus a tryptic map of recombinant DNA derived human Tissue Plasminogen Activator was explored. In order to

clarify the temperature effects and further investigate the selectivity effects, a tryptic digest of rTPA was run a series of applied voltages ranging from  $-20$  kV to  $+20$  kV. The resulting total ion currents are shown in Fig. 11. As expected, the application of voltage universally results in reduced retention. In addition, close inspection will reveal a number of regions of modified selectivity. Fig. 12 shows a plot of the differences in retention time relative to zero applied voltage as a function of applied voltage for a series of peptides and glycopeptides. If the variations in retention were due solely to temperature effects, these curves would appear symmetrical about zero applied voltage. The electrophoretic effect can be

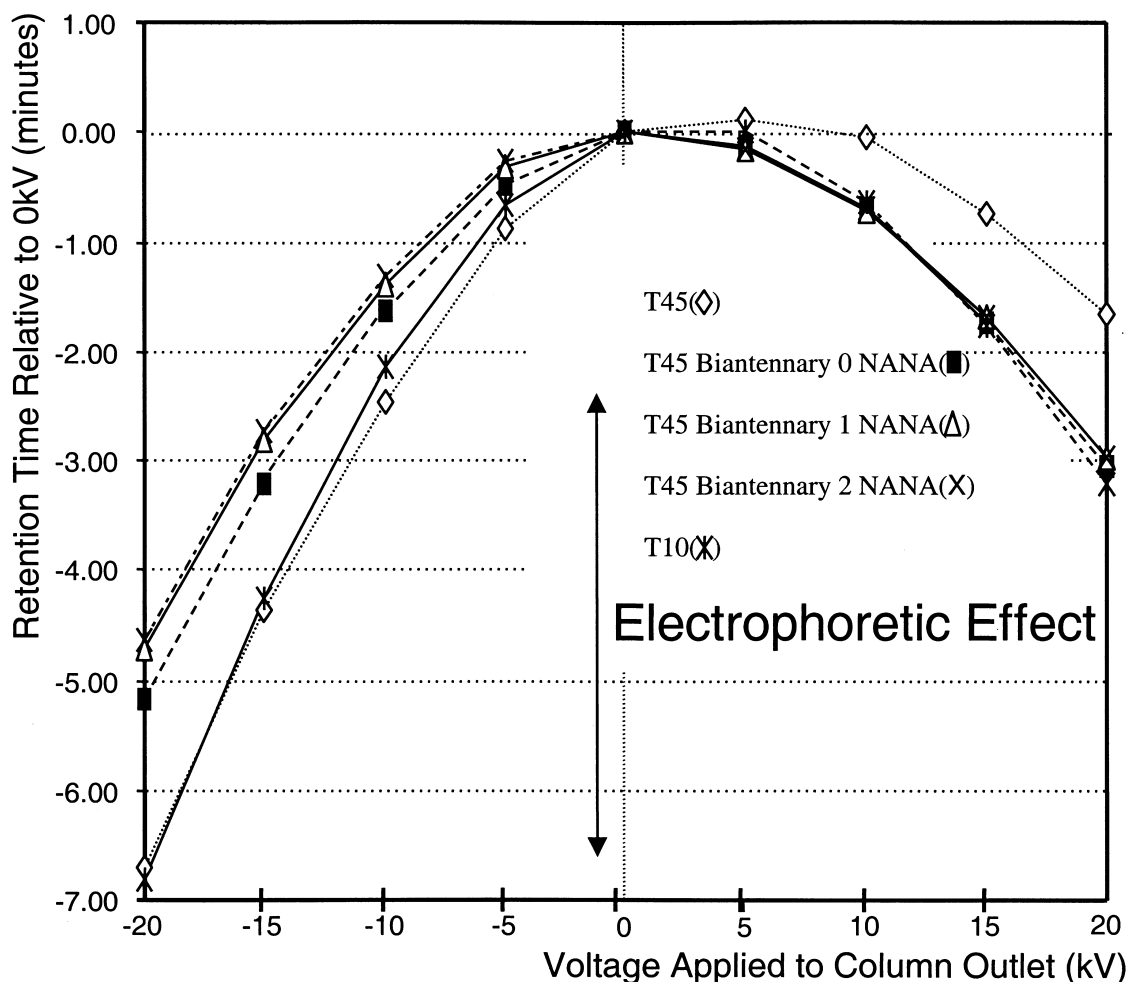


Fig. 12. Effects of voltage on retention time for selected peptides in tryptic digest of rTPA by electrically assisted cLC-MS.

determined by the difference in retention between +X kV and -X kV for a specific analyte and a specific applied voltage.

$$\mu_{\Delta} = t_{r(+kV)} - t_{r(-kV)} \quad (3)$$

It is also interesting to notice that the curves cross each other as a function of voltage, which implies significant changes in selectivity. The electrophoretic mobility under CE conditions can be predicted [10] according to the equation:

$$\mu = kZM^{-x} \quad (4)$$

where  $Z$  is the charge on the peptide,  $M$  is the mass of the peptide and  $k$  and  $x$  are constants. For this analysis, the charge on the peptide was calculated for pH 2.0 as a function of sequence using the GPMW software program [11]. Predicted mobility was calculated by fitting the data from the TPA tryptic map to Eq. (3) using the constants  $k$  and  $x$  as variable parameters. Interestingly, the optimum fit utilized a  $x$  value of 0.5 which has been suggested elsewhere as

Table 1  
Selectivity as a function of voltage

ID	Tryptic fragment	Sequence	Charge (@pH 2.0)	Mass	Differential mobility ( $\mu_d$ )	Predicted mobility ( $\mu$ )
T1	(1–7)	SYQVI CR	1.66	925.4	5.2	4.33
T3	(11–27)	TQMIY QQHQS WLRPV LR	3.66	2184.1	5.5	6.12
T4	(28–30)	SNR	1.67	375.2	7.2	6.95
T5	(31–40)	VEYCW CNSGR	1.66	1331.5	5.2	3.59
T6	(41–49)	QCHS VPVK	2.66	1025.5	5.2	6.58
T7	(50–55)	SCSEP R	1.66	735.3	5.0	4.88
T8	(56–82)	CFNGG TCQQ LYFSD FVCQC PEGF GK	1.66	3153.2	2.7	2.30
T9	(83–89)	CCEID TR	1.66	954.3	4.7	4.26
T10	(90–101)	TCYE DQGIS YR	1.66	1462.6	3.7	3.42
T12	(130–135)	RPD I R	2.66	726.4	6.8	7.86
T13	(136–145)	LGLGN HNYCR	2.66	1203.6	5.7	6.06
T15	(150–159)	DSKPW CYVFK	2.66	1329.6	6.2	5.75
T18	(190–212)	GTHSL TESG SCLPW NSMIL IGK	2.66	2460.2	4.6	4.19
T19	(213–228)	VYT Q NPS Q LGLG K	1.66	1616.9	3.4	3.25
T20	(229–233)	HNYCR	2.66	749.3	7.1	7.74
T21	(234–247)	NPDGD KPWC HVLK	3.64	1636.8	6.0	7.07
T24	(251–267)	LTWEY CDVPS CSTCG LR	1.66	2106.8	3.2	2.83
T25	(268–275)	QYSQP QFR	1.66	1052.5	4.7	4.05
T27	(278–296)	GGLF DI SH PWQ IF K	2.66	2000	5.1	4.66
T30	(300–304)	SPGER	1.66	544.3	5.8	5.70
T34	(343–351)	VVPGE EEQK	1.66	1013.5	3.7	4.13
T35	(352–356)	FEVEK	1.66	650.3	6.6	5.20
T36	(357–361)	YIVHK	2.66	658.4	7.5	8.27
T37	(362–378)	EFDDD TYDND I LLQ LK	1.66	2027.9	3.7	2.89
T39	(384–392)	C QES SVVR	1.66	1035.5	4.0	4.09
T40	(393–416)	TVCLP P DLQ LPDWT ECELS GYGK	1.66	2751.3	2.8	2.47
T41	(417–427)	HE LS PFYSE R	2.66	1334.6	6.2	5.74
T43	(430–434)	E HVR	2.66	610.3	7.6	8.61
T44	(435–440)	LYPSS R	1.66	721.4	5.1	4.93
T46	(450–462)	TVTND MLC G DTR	1.66	1453.6	4.1	3.43
T47	(463–489)	SGGPQ NLHD CQGD SGGPL VCLND GR	2.66	2754.2	3.2	3.95
T48	(490–505)	MTLVG IISWG LGCGQ K	1.66	1719.9	5.9	3.14
T49	(506–513)	DVPGV YTK	1.66	877.5	5.0	4.45
T50	(514–522)	VTNYL DWIR	1.66	1178.6	6.3	3.82
T45B0N			2.66	2898.8	2.2	3.85
T45B1N			1.66	3190.16	1.8	2.28
T45B2N			0.66	3481.42	1.73	0.87

appropriated as a shape factor related to radius of gyration for this class of solutes. A summary of these results is shown in Table 1. Fig. 13 shows a plot of  $\mu_{\Delta}$  versus  $kZ/M^{-0.5}$  for this data. The normal residual distribution (not shown) indicates that the error is due to variations unrelated (and unexplained) by the model. Although the fit is not perfect, qualitatively the behaviour is consistent. For higher charge/mass ratios, the effect is more pronounced, independent of the chromatographic characteristics of the peptide. For example, T8, a large (3153 Da) peptide with only two basic sites (including the *N*-terminus) is not effected very much by the application of a electrical potential, whereas T4 a small (375 Da) peptide with two basic sites and T3, a larger (2184 Da) peptide with total internal basic residues in addition to the basic C-terminal cleavage site and the *N*-terminus (total four) undergo signifi-

cant electrophoretic effects. The analysis of a recombinant DNA derived protein expressed in CHO cells is complicated by the glycosylation that typically displays a high degree of microheterogeneity. For rTPA, for example, it has been calculated that including all three *N*-linked glycosylation sites there is a possibility of 11,520 different glycoforms present in varying abundances. It is interesting to note that the three glycoforms of peptide T45, which contains the third glycosylation site, differ only by the sequential addition of zero, one and two sialic acids do not behave according to the model. This is not surprising since the addition of the carbohydrate moiety will significantly effect the hydrodynamic volume of the glycopeptide. Furthermore, the addition of constituent sialic acid results in a pronounced electrophoretic mobility effect which actually reverses the elution order as shown in Fig. 14. These

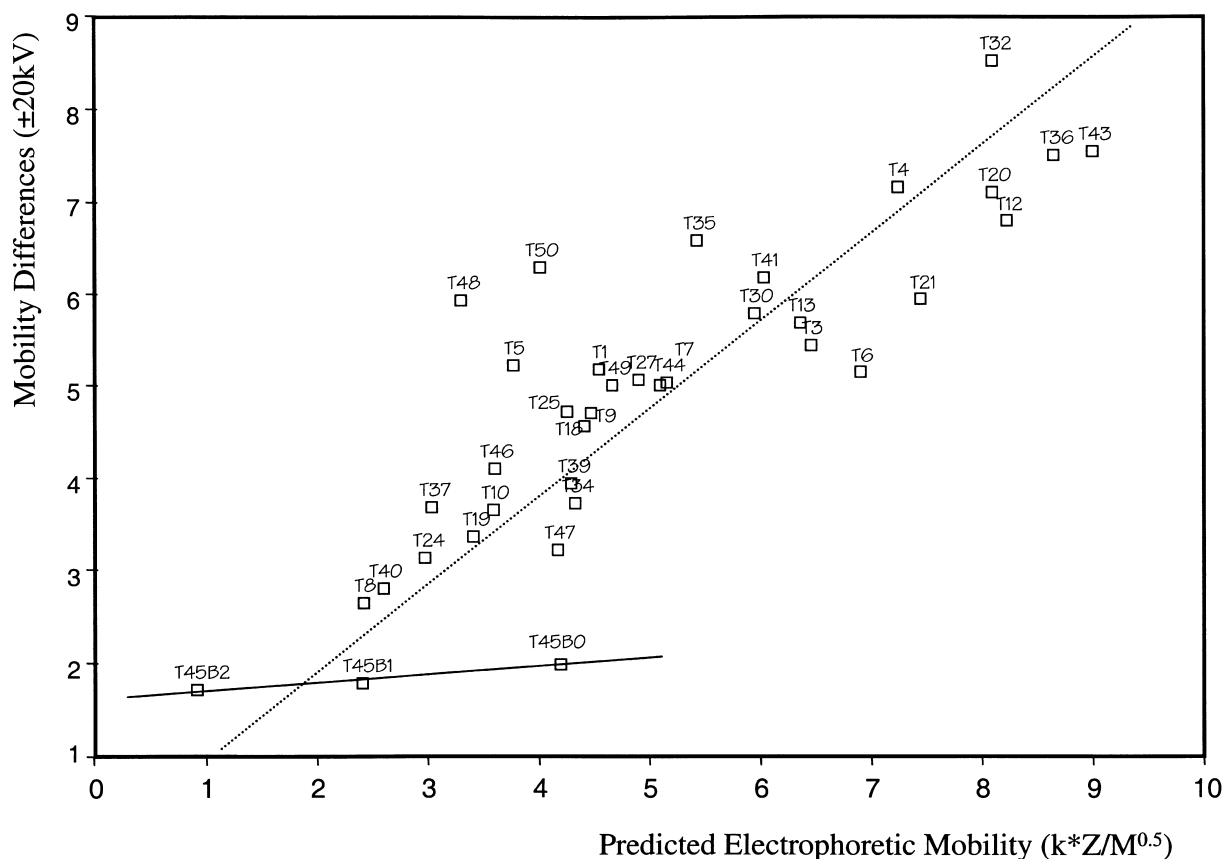


Fig. 13. Predicted mobility effects versus observed shifts in HPLC retention due to applied voltage.

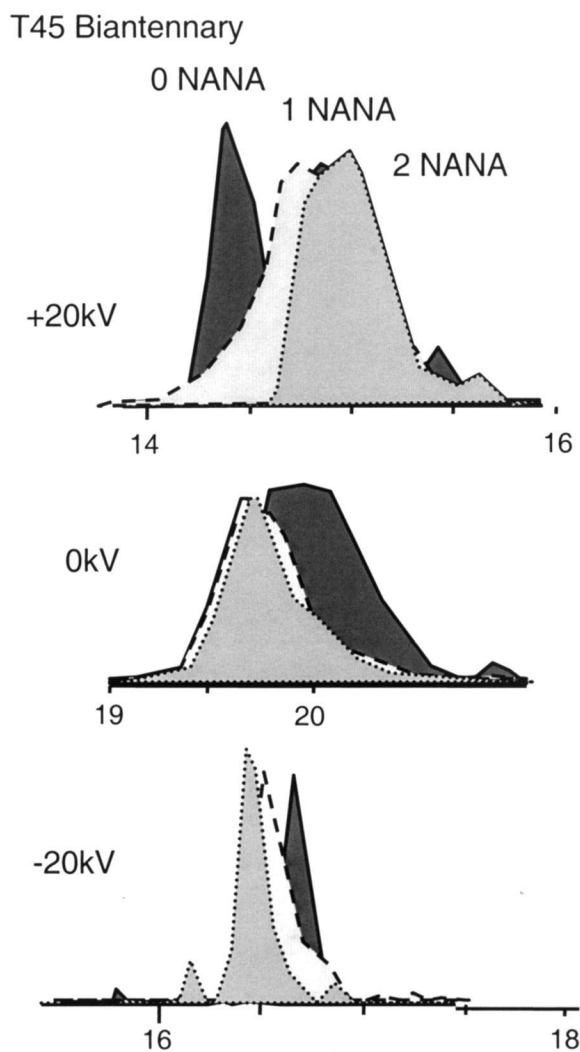


Fig. 14. Effect of applied voltage on glycoprotein separation in tryptic digest of rTPA by electrically assisted cLC-MS.

results indicate that the use of radial electrical fields may be helpful in the analysis of complex glycoprotein peptide maps.

Lack of fit in Fig. 13 can be attributed to number of factors. In terms of the experimental conditions, as was described above, the capillary column was not thermostatted and while comparison of positive and negative voltage experiments of the same absolute magnitude accounts for joule heating effects, it does not address uncontrolled temperature variations. In terms of the generation of the model, the approxi-

mation of the charge values for the individual peptides depends on the determination of the pH value of the solvent. While pH 2.0 is the appropriate value for 0.2% aqueous TFA, the addition of organic solvent during the gradient will tend to shift this to higher effective pH [12].

#### 4. Conclusions

A system has been developed and demonstrated that allows capillary separation in a variety of modes including capillary electrophoresis, capillary HPLC, capillary electrochromatography (CEC), gradient CEC and electrically assisted capillary HPLC. This system, utilizing electrically assisted capillary HPLC has been interfaced with electrospray LC-MS to investigate selectivity effects in peptide separations. In the separation of tryptic digests of recombinant DNA derived human growth hormone (rGH) and tissue plasminogen activator (rTPA), it was found that although gradient elution reversed-phase separation mechanisms dominate the separation, there is a small, but significant contribution to selectivity due to the imposed electrical potential that can be used to fine tune a separation.

In on-going work, we plan to improve the operational characteristics of the electrically assisted cLC-MS interface to accommodate temperature control and to better optimize extracolumn dispersion effects in the interface.

#### Acknowledgements

The authors gratefully acknowledge John Frenz and Billy Wu of Genentech, Inc. for the supply of hGH and TPA samples.

#### References

- [1] M.M. Dittman, K. Wienand, F. Bek, G.P. Rozing, *LC-GC* 10 (1995) 802.
- [2] J.H. Knox, I.H. Grant, *Chromatographia* 32 (1991) 317.
- [3] N.W. Smith, M.B. Evans, *Chromatographia* 38 (1994) 649–657.
- [4] A. Apffel, S. Fischer, G. Goldberg, P.C. Goodley, F.E. Kuhlmann, *J. Chromatogr. A* 712 (1995) 177–190.

- [5] A. Apffel, P.G. Goodley, S. Fischer, J. Bertsch, M. Wehrlick, Presented at the 13<sup>th</sup> Montreux Symposium on Liquid Chromatography–Mass Spectrometry, Montreux, 13–15 November, 1996.
- [6] L.E. Snyder, J.J. Kirkland, Introduction to Modern Liquid Chromatography, 2nd ed., Wiley, New York, 1979, p. 665.
- [7] M.-I. Aguilar, M.T. Hearn, Methods Enzymol. 270 (1996) 3.
- [8] W.S. Hancock, R.C. Chloupek, J.J. Kirkland, L.R. Snyder, J. Chromatogr. A 686 (1994) 31–43.
- [9] R.C. Chloupek, W.S. Hancock, B.A. Marchylo, J.J. Kirkland, B.E. Boyes, L.R. Snyder, J. Chromatogr. A 686 (1994) 45–59.
- [10] R.E. Offord, Nature 211 (1966) 591.
- [11] GPMAW, Ver 3.02, Lighthouse Data 1997.
- [12] F.M. Rabel, D.J. Popovich, Am. Chem. Soc. Abstr. 77 197 (1979) 401.